

AD-A016 192

SHOCK WAVE PROPAGATION IN AN INHOMOGENEOUS MEDIUM
USING FINITE DIFFERENCES

D. G. Colombant, et al

Naval Research Laboratory

Prepared for:

Defense Nuclear Agency

September 1975

DISTRIBUTED BY:

NTIS

National Technical Information Service
U. S. DEPARTMENT OF COMMERCE

ADA016192

Shock Wave Propagation in an Inhomogeneous Medium Using Finite Differences

D. G. COLOMBANT

*Science Applications, Inc.
McLean, Virginia 22101*

and

J. H. GARDNER

*Plasma Dynamics Branch
Plasma Physics Division*

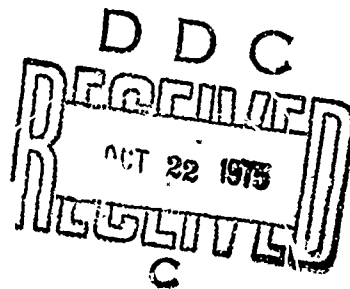
September 1975

This research was sponsored by the Defense Nuclear Agency under Subtask S91QAXHC062, work unit 34, and work unit title Phenomenology Affecting Satellite Communications.



Reproduced by
NATIONAL TECHNICAL
INFORMATION SERVICE
US Department of Commerce
Springfield, VA. 22151

NAVAL RESEARCH LABORATORY
Washington, D.C.



REPORT DOCUMENTATION PAGE		READ INSTRUCTIONS BEFORE COMPLETING FORM
1. REPORT NUMBER NRL Memorandum Report 3116	2. GOVT ACCESSION NO.	3. RECIPIENT'S CATALOG NUMBER
4. TITLE (and Subtitle) SHOCK WAVE PROPAGATION IN AN INHOMOGENEOUS MEDIUM USING FINITE DIFFERENCES		3. TYPE OF REPORT & PERIOD COVERED Interim report on a continuing NRL problem.
		4. PERFORMING ORG. REPORT NUMBER
7. AUTHOR(s) D. G. Colombant and J. H. Gardner		5. CONTRACT OR GRANT NUMBER(s)
9. PERFORMING ORGANIZATION NAME AND ADDRESS Naval Research Laboratory Washington, D.C. 20375		10. PROGRAM ELEMENT, PROJECT, TASK AREA & WORK UNIT NUMBERS NRL Problem H02-27E DNA Subtask HC062
11. CONTROLLING OFFICE NAME AND ADDRESS Defense Nuclear Agency Washington, D.C. 20305		12. REPORT DATE September 1975
		13. NUMBER OF PAGES 33
14. MONITORING AGENCY NAME & ADDRESS (if different from Controlling Office)		15. SECURITY CLASS. (of this report) UNCLASSIFIED
		15a. DECLASSIFICATION/DOWNGRADING SCHEDULE
16. DISTRIBUTION STATEMENT (of this Report) Approved for public release; distribution unlimited.		
17. DISTRIBUTION STATEMENT (of the abstract entered in Block 20, if different from Report)		
18. SUPPLEMENTARY NOTES This research was sponsored by the Defense Nuclear Agency under Subtask S99QAXHC062, work unit 34, and work unit title Phenomenology Affecting Satellite Communications.		
19. KEY WORDS (Continue on reverse side if necessary and identify by block number) Shock wave Inhomogeneous medium Numerical Hydrodynamic		
20. ABSTRACT (Continue on reverse side if necessary and identify by block number) One-dimensional propagation of a strong shock wave in a medium with an exponentially varying density is studied numerically. Solutions using various formulations of the energy equation are compared with the self-similar analytic solution. It was found that only the conservative energy equation predicts the correct shock propagation; the temperature and pressure formulations, even with artificial viscosity are far less satisfactory. This result holds over a wide range of different spatial resolutions and for different finite-difference algorithms.		

CONTENTS

Section 1 — INTRODUCTION	1
Section 2 — RESULTS FOR THE INCREASING DENSITY CASE ...	6
Variations of the Results with Grid Size	8
Section 3 — RESULTS FOR DECREASING DENSITY CASE	10
Section 4 — CONCLUSIONS	13
ACKNOWLEDGMENTS	14
REFERENCES	14

SHOCK WAVE PROPAGATION IN AN INHOMOGENEOUS MEDIUM USING FINITE DIFFERENCES

Section 1

INTRODUCTION

Finite-difference fluid equations have been known¹⁻⁴ to provide valid solutions to problems containing shocks when the physically correct conservation variables in conservation form are used. In this study, we examine the problem of shock propagation in an inhomogeneous medium with exponentially varying density. The one-dimensional self-similar analytic solution to this problem will be compared to various numerical solutions using different algorithms. This problem constitutes a more severe numerical test for shock propagation than the shock wave in an homogeneous medium and therefore serves as a better test of numerical algorithms.

In particular we find that care must be taken in the use of forms of the hydrodynamic equations which do not express physical conservation. For non-conservation formulations of the energy equation an artificial viscosity must be introduced, not only to provide the necessary stability, but also to provide shock heating. The magnitude of this artificial viscosity to obtain best shock results depends on the grid size and the problem type. There is no simple way to obtain this optimal viscosity for problems where the solution is not known in advance.

In addition, we find that Flux-Corrected Transport⁵ (FCT) has several properties which make it more flexible and effective for shock calculations. While the comparison between different energy formulations has been made easier through the use of the FCT scheme, the results hold for any finite difference algorithm and in particular they will be shown to hold using the Lax-Wendroff scheme as well.

Note: Manuscript submitted August 22, 1975.

The problem and its analytical solution are well described by Zeldovich and Raizer.⁶ We outline here their self-similar solution as well as the conditions under which it holds. The solution is given both for the increasing and decreasing density cases. The medium is defined by its characteristic length - or scale height - which is equal to the e-folding distance. The analytic solution is given as a function of the similarity variable ξ which is equal to $\frac{X - x}{\Delta}$ where X is the shock location and x is the Eulerian coordinate location. The velocity of the shock front is given by $D = \alpha \frac{\Delta}{t}$ where α - a coefficient which depends only on the specific heat ratio γ - is determined by the solution of a boundary-value problem.⁶ For the increasing density problem with $\gamma = 2$ ($\alpha = 1.5$), the self similar analytic solution behind the shock is:

$$\begin{aligned}\rho &= \frac{\gamma+1}{\gamma-1} \rho_0(X) (1+2\xi)^{-5/2} \\ p &= \frac{2}{\gamma+1} \alpha^2 \frac{\Delta^2}{t^2} \rho_0(X) (1+2\xi)^{-3/2} \\ u &= \frac{2}{\gamma+1} \alpha \frac{\Delta}{t} (1-\xi)\end{aligned}$$

where $\rho_0(X)$ is the ambient density immediately in front of the shock. The unperturbed medium is characterized by

$$\begin{cases} \rho = \rho_0(X) e^{-\xi} \\ p = 0 \\ u = 0 \end{cases}$$

The initial conditions for our calculations were also taken after the self-similar solution had developed. The only restriction on the application of the analytic solution is that the initial pressure and temperature be taken equal to 0. While this condition is difficult to satisfy rigorously in a numerical calculation, the temperature and

the pressure of the ambient gas have been chosen to be very small so that the pressure and temperature ratios across the shock are very large (5×10^4 typically for the pressure ratio). This corresponds to the infinite Mach number, strong shock limit required for the self-similar solution.

Three different variables have been used for the energy equation, while the continuity and momentum equations have been treated in their usual conservative form. The numerical algorithms used treat all conservative terms in conservative finite-difference form. Use has been made of a Lax-Wendroff scheme (LW) and a Flux-Corrected Transport (FCT) scheme. The Lax-Wendroff scheme uses the two-step Richtmeyer form coupled with a Von Neumann viscosity to provide the additional stability and viscous heating needed near the shocks. The FCT scheme makes use of artificial viscosity (Von Neumann type) when the energy equation is cast in terms of the pressure or temperature variable, to provide the viscous heating otherwise lacking in the shocks. Artificial viscosity is not needed in the strict conservative formulation.

The first set of equations used solves for the mass, momentum, and total energy per unit volume and is in strict conservative form. The second set is based on mass, momentum, and pressure whereas the last one uses mass, momentum, and temperature. The total energy, pressure, and temperature equations are respectively:

$$\frac{\partial E}{\partial t} + \underline{\nabla} \cdot \underline{v} E = - \underline{\nabla} \cdot (p + q) \underline{v} \quad (1)$$

$$\frac{\partial p}{\partial t} + \underline{\nabla} \cdot \underline{v} p = - (\gamma - 1)(p + q) \underline{\nabla} \cdot \underline{v} \quad (2)$$

$$\frac{\partial T}{\partial t} + \underline{\nabla} \cdot \underline{v} T = - [(\gamma - 2)T + (\gamma - 1) \frac{q}{\rho}] \underline{\nabla} \cdot \underline{v} \quad (3)$$

$$q = -\rho b(\epsilon x^2) \left| \frac{\partial u}{\partial x} \right| \frac{\partial u}{\partial x} \quad (4)$$

where $E = \rho(\epsilon + \frac{1}{2} v^2)$ and $\epsilon = \frac{p}{(\gamma-1)\rho}$ for a perfect gas.

The conservation form of the difference equations is a necessary but not a sufficient condition to guarantee the correct weak (discontinuous) solution to the ideal hydrodynamic equations. It is possible to get different weak solutions by using different equivalent forms of the partial differential equations. The jump conditions depend on the form of the equation and we must use physical reasoning to determine if these jump conditions make sense. In dealing with physical laws we usually try to write the equations in a conservation form which implies actual physical conservation. In hydrodynamics only the total energy equation combined with the mass and momentum equation provides a consistent set of equations for physically conserved quantities.

This problem of correctly calculating the weak solutions can be avoided by introducing viscosity and seeking genuine (continuous) solutions. With viscosity the hydrodynamic equations do not have truly discontinuous solutions and all forms of the energy equation should be equivalent. Artificial viscosities - and not real viscosity - have to be added to provide the necessary heating because real viscosity acts over a few mean free paths which are usually much smaller than the grid size. The effect of a real physical viscosity will always be too small unless the mean free path and cell size are comparable. However, the difficulty with artificial viscosity is that the shock

profile must be spread over several cells for stability regardless of the actual physical thickness of the shock and thus interactions of the shock with inhomogeneous media will not be accurate unless the background varies slowly. Further, since there is little physical basis for the artificial viscosity, we can only hope that it will produce the correct heating in non-conservative formulations.

In this regard the FCT finite difference formulation seems to have a distinct advantage in that its shock profile spreads over only a couple of cell widths almost independent of the coefficient used for the artificial viscosity. The velocity gradient used in the Von Neumann viscosity is nearly independent of the coefficient and thus any amount of heating that is desired can be achieved by raising the viscosity coefficient. In most other schemes the larger coefficient tends to smooth out the shock profile which reduces the velocity gradient and somewhat offsets the effect of increased coefficient.

It is the failure to compute accurately the dissipation mechanism which converts kinetic energy to thermal energy that leads to a failure to conserve energy in the temperature and pressure formulations and hence gives incorrect results for the shock dynamics. Since the total energy equation is in divergence form whether the viscosity terms are included or not, conservation of energy is automatically guaranteed when a conservative difference scheme is applied to it. In the remainder of the paper we will show the results of several test calculations demonstrating these ideas. Section Two shows the results for a shock propagating into an exponentially increasing density medium. The results of the different formulations are compared for several values of the artificial viscosity parameters and grid sizes. In Section Three the results for the decreasing density case are shown and in Section Four the conclusions that can be drawn from this study are made.

Section 2

RESULTS FOR THE INCREASING DENSITY CASE

For a $\gamma=2$ gas the self-similar solution is completely analytic. From the Rankine-Hugoniot relations, we expect the density jump across the shock to be equal to 3. Figures 1 and 2 show density profiles for the energy and temperature equations respectively for the LW scheme after a time $t=350 \delta t$. At that time, the shock has moved over a distance equal to 1.3Δ . Three different values of the viscosity coefficient have been used and the effect of non-conservation is shown clearly from these two figures. In the total energy formulation, the value of b affects mainly the stability of the solution (and the amplitude of the ripples behind the shock); in the temperature formulation, it changes the speed of propagation of the shock significantly. For the latter equation, the larger the viscosity coefficient, the more the viscous heating and the better the agreement between the numerical solution and the analytic solution. Note, however, that the peak density behind the shock decreases with the artificial viscosity coefficient b and thus the density profiles cannot be taken as the only criteria of good numerical solutions.

The integrated total and thermal energies are shown in Figure 3 for some of these cases. This figure shows that energy conservation is better achieved by using the total energy formulation. Note that while for the correct energy conserving formulation the integrated thermal energy is increasing with time, in the case of the temperature formulation it is actually decreasing. As

we have seen, this loss of thermal energy reduces the driving force of the shock and results in the shock lagging the correct solution. When the temperature equation is used, energy conservation is improved by increasing the magnitude of the artificial viscosity coefficient. A limiting case occurs when the b coefficient in q is sufficiently large to make the artificial pressure greater than the real pressure in the shock front. In that case, too much heat is generated in the shock and, for example by using $b=4$ in the FCT temperature scheme the shock moves faster than its analytic counterpart by 1%. The total integrated energy also increases above its correct value for this case and the difference reaches 1.8% at the end of the run. Note also that for these cases the stability requires a smaller time step since both the temperature and the shock velocity take larger values than in a real shock.

Another limiting case is shown in Figure 4 where q has been set equal to 0 for both the temperature and the pressure equation formulation. The algorithm used in this case is FCT since LW would be unstable. The shock lags behind its exact solution to a much larger extent than shown previously and 36% of the total energy is lost using this formulation.

It was investigated whether these results depend on the form of the artificial viscosity coefficient. In Figure 5, use has been made of the Tyler viscosity coefficient⁷ with the LW scheme using the temperature formulation. The density profiles look smoother than for the Von Neumann viscosity but the energy conservation is not as good and consequently the shock location is also worse. Once again, smooth density profiles do not constitute a complete criterion for good numerical solutions. The shock dynamics, which can be checked only against an exact solution, must also be considered.

Variations of the Results with Grid Size

Results shown previously have been obtained with a fixed grid size corresponding to a spatial resolution of 40 grid points per scale height. In practice, the resolution is often much coarser so the influence of the spatial resolution on the results is now investigated. Figure 6 shows the results for the density profiles when the grid size δx is multiplied by 4 so the scale height is made up of 10 grid points; the density profile in the shock broadens and the peak value of the density just behind the shock decreases. For this kind of spatial resolution, all equations have difficulty in simulating the presence of a strong shock and in fact look similar. The two-cell-wide flat top on the density profile is characteristic of FCT⁸. The energy equation, although showing a reduced density ratio across the shock, still approximates fairly well the shock location and yields energy conservation. The two other energy equation formulations gain energy by 10% to 16% with the pressure equation more nearly conserving energy. These results contrast with the finer resolution cases for which the same values of b lead to a loss of energy. Although the effect of grid size is supposed to be scaled out of the problem by the form of the artificial viscosity used, in effect when the non-conservative formulations are used energy conservation and shock location are altered by changes in grid resolution even when the same coefficient of artificial viscosity is used. Clearly, for this resolution, information about the shock has been mostly lost for both temperature and pressure equations and suggests that even 10 grid points per scale height with the energy equation represents a minimum resolution in order to provide a meaningful solution.

Figure 7 shows density profiles for the temperature equation when the spatial resolution has been increased to 80 cells per scale height. The shock width decreases while the density jump ratio

increases for the same value of the parameter b in the artificial viscosity coefficient.

From the results presented for the increasing density case, it is apparent that only the total energy equation formulation yields a correct result in which the shock location does not depend strongly on the viscosity coefficient or on changes in the grid size. For the other energy equation formulations, although it is possible to find an optimum value for the viscosity coefficient in each specific case, this value is not independent of changes in grid size or problem parameters. The total energy equation is thus superior in all respects to the non-conservative forms. Although this result is already known⁴, attempts to use the non-conservative formulation with (or even without) artificial viscosity for viscous heating in shocks have been made repeatedly. Further, this work has allowed us to quantify this notion for a specific case by estimating the error made when a non-conservative form is used.

Section 3

RESULTS FOR DECREASING DENSITY CASE

In case of an exponentially decreasing density medium, the "analytic" self-similar solution does not exist and has to be replaced by the numerical solution of the following ordinary differential equations:

$$\frac{dp}{d\eta} = \frac{\gamma+1}{2\alpha} \frac{1 - \frac{\gamma-1}{\gamma+1} \left(1 - \frac{2-\alpha}{\gamma}\right) p^{-1/\gamma} \eta^{-(2-\alpha)/\alpha\gamma}}{1 - \frac{\gamma-1}{2\gamma} p^{-(1/\gamma)-1} \eta^{1-(2-\alpha)/\alpha\gamma}}$$

$$\tilde{p} \tilde{\rho}^{-\gamma} \eta^{(2/\alpha)+\gamma-1} = 1$$

$$\tilde{n} + \alpha \eta \frac{d\tilde{u}}{d\eta} = \alpha \frac{d\tilde{p}}{d\eta}$$

$$d\eta = - \frac{\gamma+1}{\gamma-1} \tilde{\rho} d\xi$$

where \tilde{u} , \tilde{p} , and $\tilde{\rho}$ is the solution behind the shock. Since the solution to these equations is well-behaved, monotonic, and does not involve computing the shock wave, good precision can be obtained and a meaningful comparison can be performed with the results of the partial differential equations used previously for the "numerical" solution. The specific heat ratio γ was chosen to be equal to 7/5 for this case ($\alpha = 5.45$) and results are summarized briefly below.

Figures 8 and 9 show the density profiles for a very strong shock propagating in a decreasing density medium for the FCT and LW schemes respectively. At the time it is shown ($t = 200\delta t$) the shock has traveled approximately a distance equal to 1.2Δ . The grid size is the same as that used in Figures 1-5. Note that this time the shock is accelerating.

Several interesting features may be noted from these graphs. First, using an artificial viscosity coefficient $b=2$ results in the shock propagating too fast for both the FCT and LW schemes. This is in contrast to the results of the increasing density case shown in Figures 2, 5, and 7 where a coefficient $b=2$ resulted in too slow a shock propagation. Again for the decreasing density case a coefficient $b=0.5$ results in the shock lagging behind the analytic solution. The $b=1$ coefficient for the LW method gives reasonable shock location but shows significant ripples behind the shock. For comparison the solution obtained with the conservation energy formulation is shown in Figure 8 and again this shock location result is in agreement with the analytic solution.

Integrated total and thermal energies can be computed as previously. The differences are much smaller for this decreasing density case (of the order of 3%) and this can easily be explained by the fact that since the shock propagates in a region of decreasing density, the energy carried by the shock represents a decreasingly smaller fraction of the total initial energy. Thus, while the energy is conserved to a much better accuracy than previously the error in the shock dynamics is not reflected as much in the total energy conservation and energy conservation is a less useful check on accuracy.

Another test shows the results obtained with a pressure equation. In general, the use of the pressure equation leads to the same kind of results as those obtained from the temperature equation. More specifically, because it involves the conservation of thermal energy, the results it yields lie between those given by the temperature and the total energy equation. The artificial viscosity coefficient is similar to that used previously and we see in this particular example

that the pressure equation, although predicting quite accurately the shock location using FCT, oscillates much more than the temperature equation. Oscillations in Figs. 8 and 9 may have different origins. They are clearly characteristic oscillations behind a shock for the LW algorithm. As for the FCT scheme, the fluctuations also seem to be characteristic⁸, but they are somewhat weaker terraces in which only the derivative oscillates.

Section 4

CONCLUSIONS

In this study, it has been shown that the numerical results obtained for shock speeds and instantaneous profile in an exponentially varying density medium can differ largely due to the choice of energy equation and spatial resolution. By comparison with an analytic solution, it has been shown that only the conservative energy equation is reliable. Even in this best case, a fairly fine spatial resolution is needed in order to derive accurate results.

The inclusion of some artificial viscosity is necessary not only for stability but to produce the necessary shock heating in the case of the temperature and pressure formulations. By suitable adjustment of the coefficient of artificial viscosity one can obtain a wide range of shock profiles and shock heating and achieve near conservation and therefore good solutions. However, it was found that there is no unique way to choose this coefficient and the precise value to achieve conservation depends both on the grid size and the nature of the problem.

The FCT algorithm does not require artificial viscosity for stability and maintains a steep profile rather independent of the value of artificial viscosity. Thus, if the temperature or pressure equation must be used, FCT gives more flexibility in achieving the correct amount of heating in the shock front. In addition, in the case of the total energy formulation, the FCT scheme requires no artificial viscosity at all, removing an additional restriction on the time step and allowing larger time steps to be used.

ACKNOWLEDGMENTS

We are indebted to Dr. S. Zalesak for lending us an updated version of FCT. We would like to acknowledge many useful discussions with Drs. D. Book and N. Winsor. Finally, we thank Dr. J. Boris for his critical remarks, helpful suggestions, and his careful reading of the manuscript.

This work was supported by the Defense Nuclear Agency.

REFERENCES

1. P. D. Lax, Comm. Pure Appl. Math. 7, 159 (1954).
2. P. D. Lax, Comm. Pure Appl. Math. 10, 537 (1957).
3. P. D. Lax and B. Wendroff, Comm. Pure Appl. Math. 13, 217 (1960).
4. J. Gary, Math. of Comp. 18, 1 (1966).
5. J. P. Boris and D. L. Book, J. Comput. Phys. 11, 38 (1973).
6. Y. B. Zeldovich and Y. P. Raizer, Physics of Shock Waves and High Temperature Phenomena, Academic Press, Vol II, p. 852-863 (1956).
7. L. D. Tyler and M. A. Ellis, "The Tshok code: Lax Version," SC-TM-70-153, Sandia Laboratories (1970).
8. D. L. Book, J. P. Boris and K. Hain, Generalization of the Flux Corrected Transport Technique, NRL Memorandum Report 3021 (1975).

TOTAL ENERGY EQUATION-LW ALGORITHM-

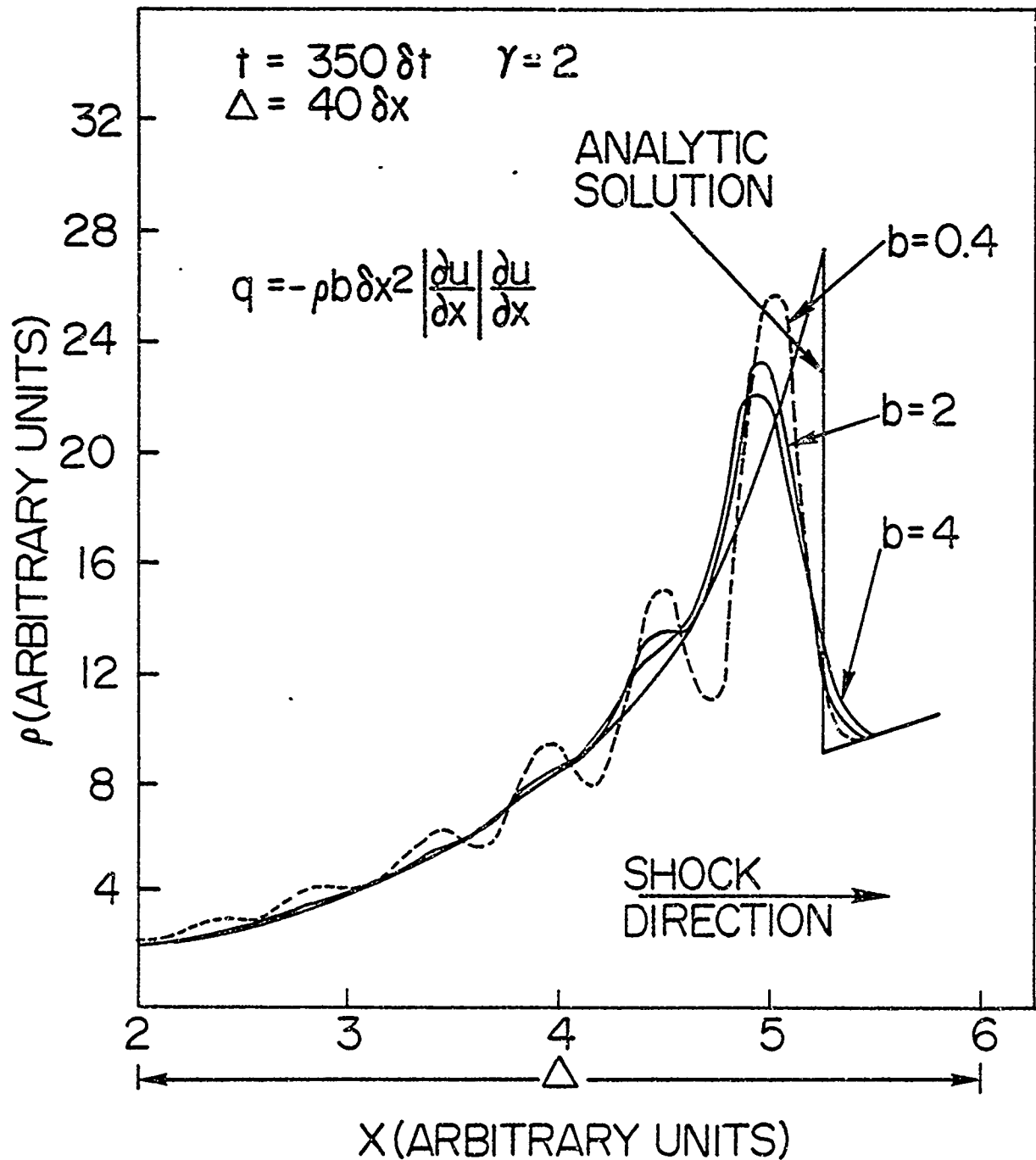


Fig. 1 — Shock density profiles for shock propagating in the increasing density direction. Total energy equation formulation with Lax-Wendroff (LW) algorithm. The shock was located at $x = 0$ at $t = 0$.

TEMPERATURE EQUATION - LW ALGORITHM -

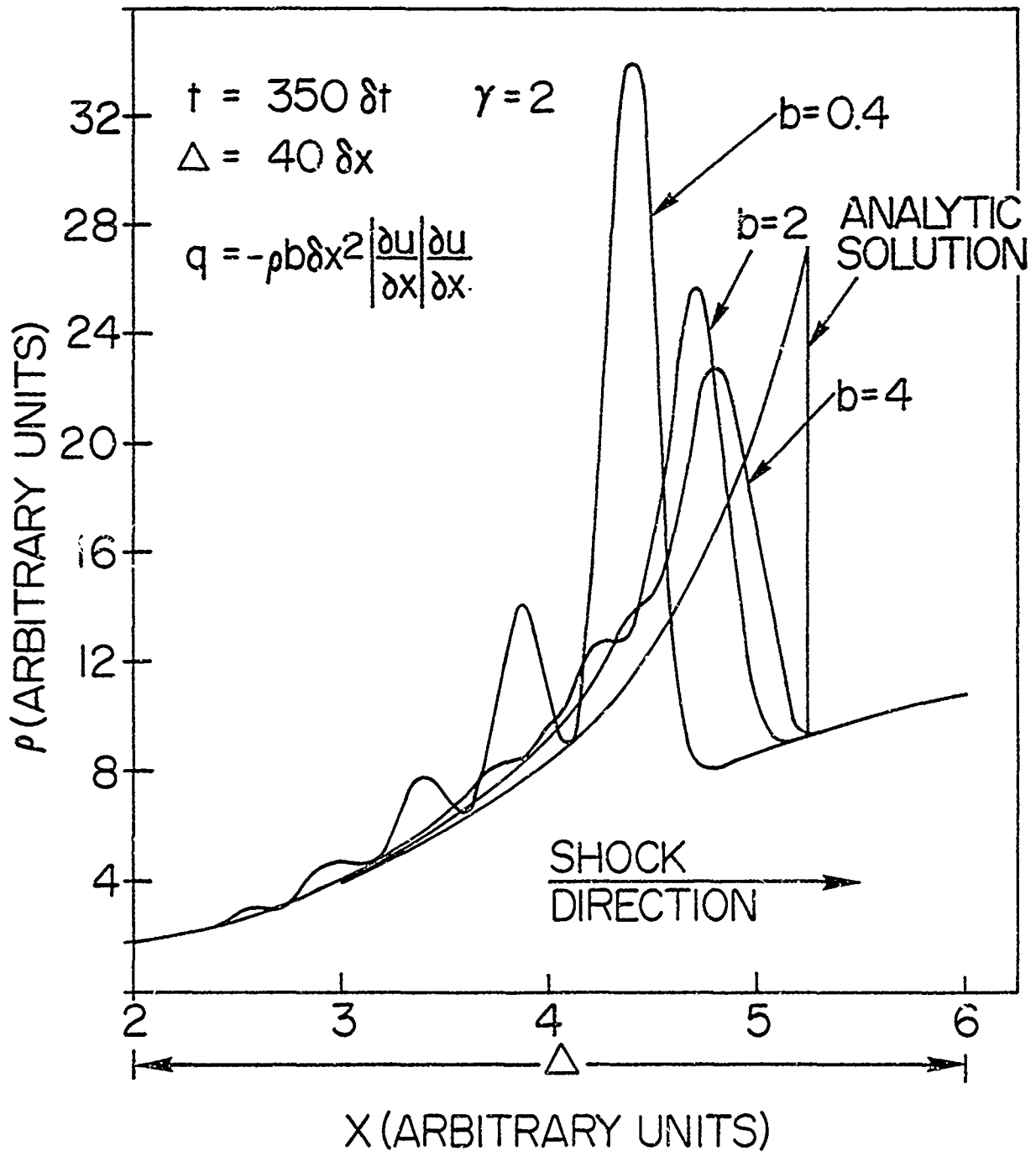


Fig. 2 — Shock density profiles corresponding to the case of Fig. 1 for temperature equation formulation

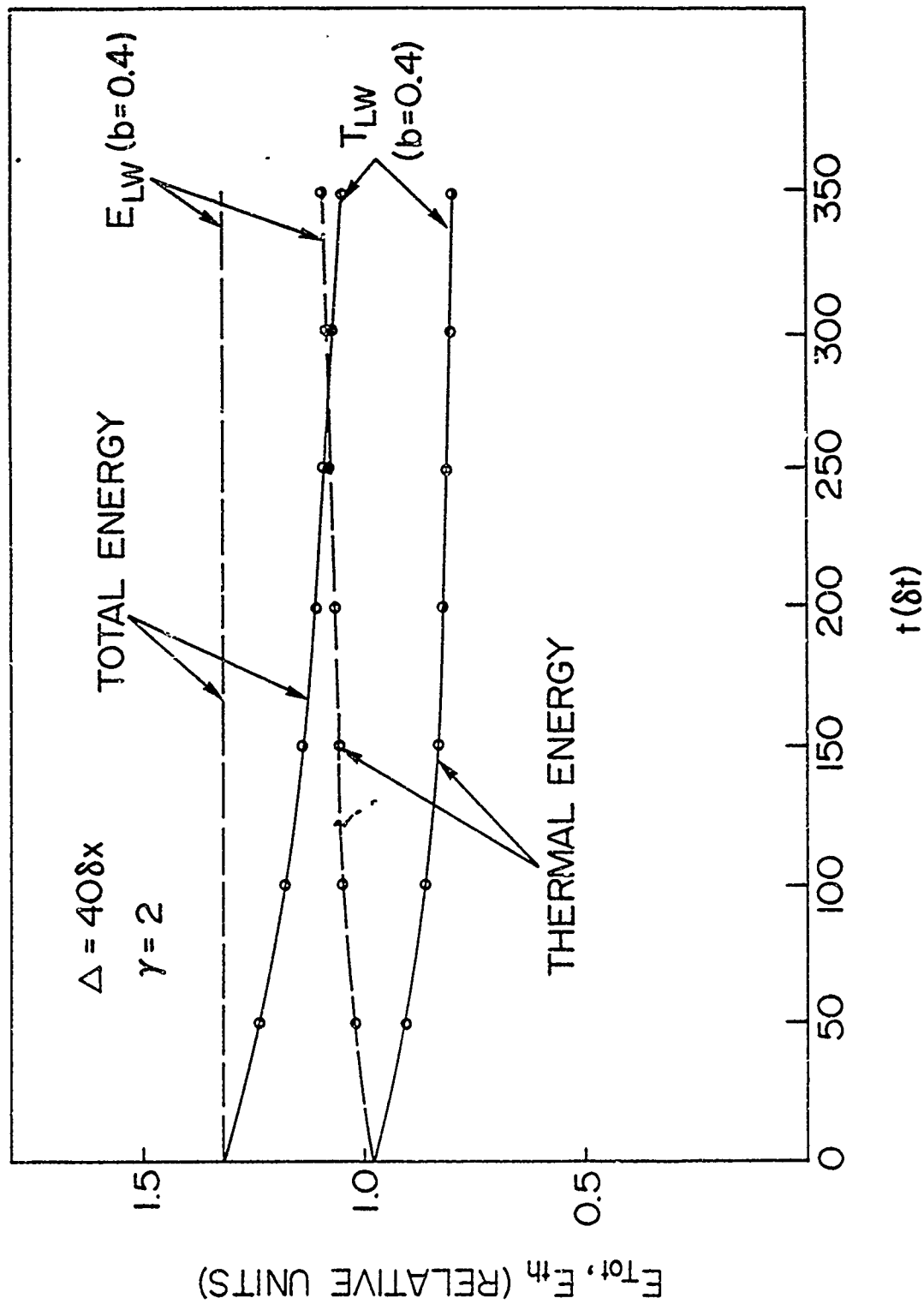


Fig. 3 — Spatially integrated total and thermal energies as a function of time for cases of Figs. 1 and 2

VARIOUS ENERGY EQUATIONS -b=0 -FCT ALGORITHM-

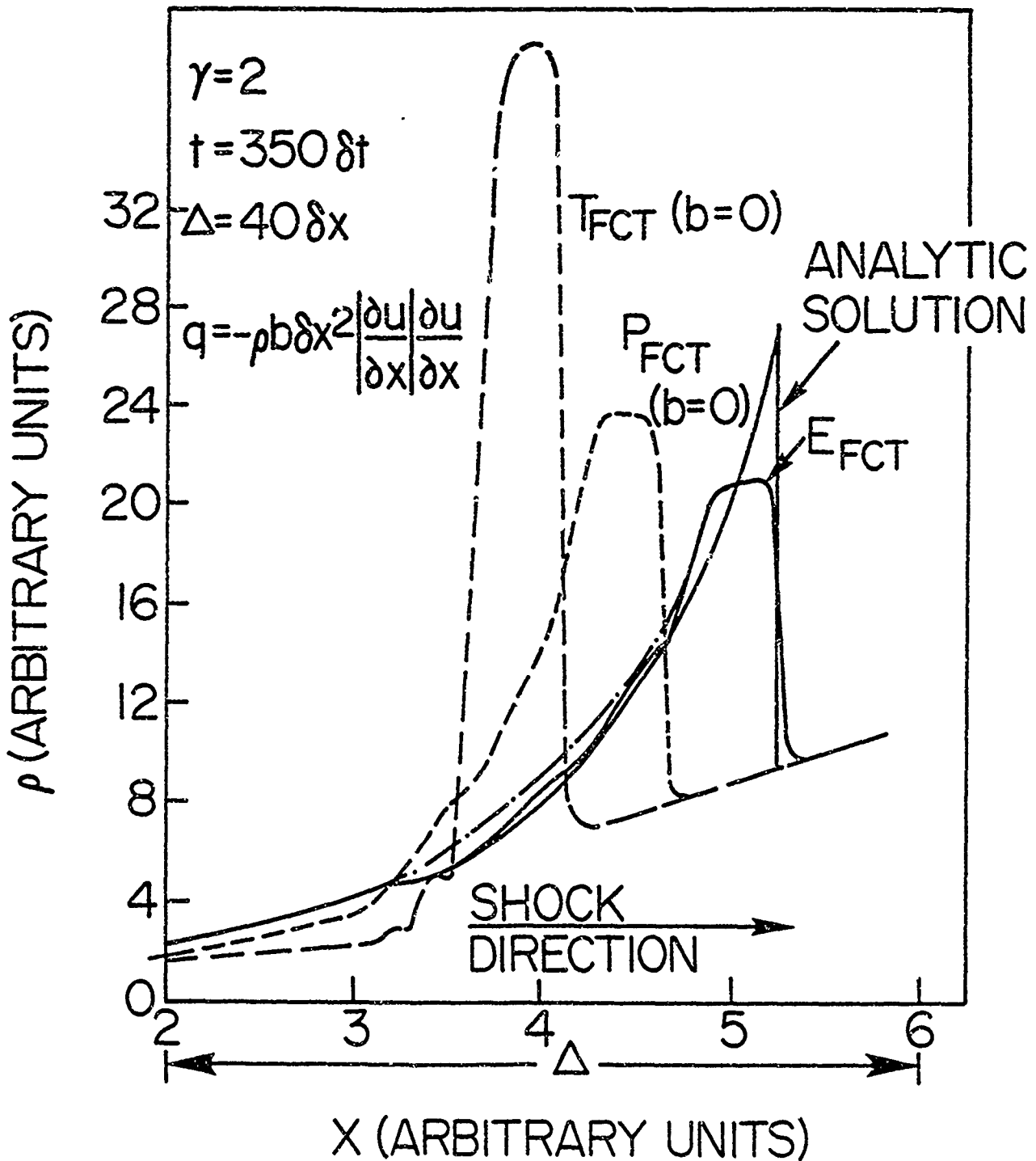


Fig. 4 — Comparison of the different energy equation formulations (energy E, temperature T, pressure P) without any artificial viscosity using Flux-Corrected Transport (FCT)

TEMPERATURE EQUATION-LW ALGORITHM-

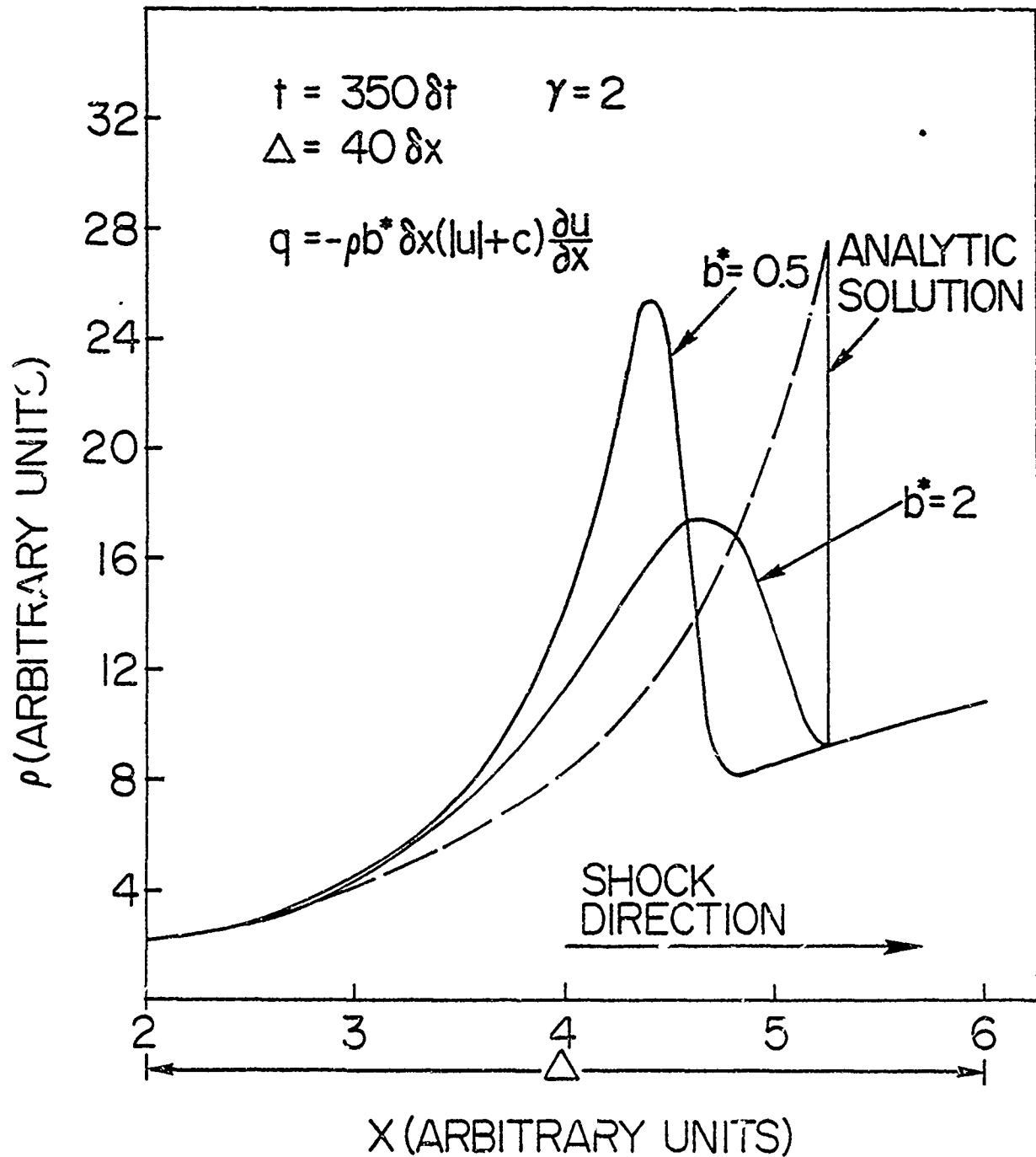


Fig. 5 — Same as Fig. 2 using Tyler's form of artificial viscosity

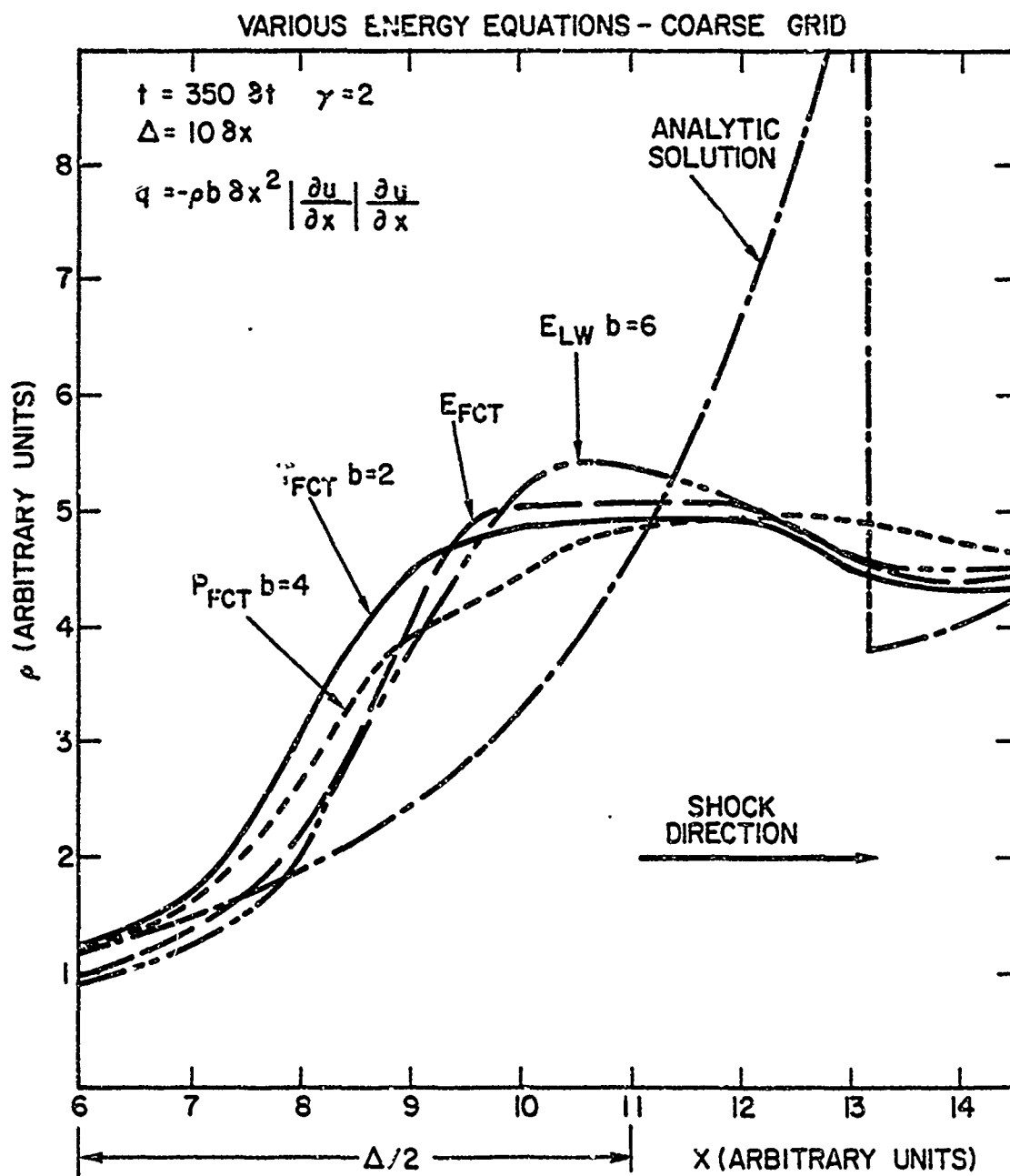


Fig. 6 -- Influence of grid size. Grid size is four times as large as for previous figures. Shock density profiles are shown for various energy equations formulations using FCT and for the total energy equation using LW(E_{LW}).

TEMPERATURE EQUATION - LW ALGORITHM -

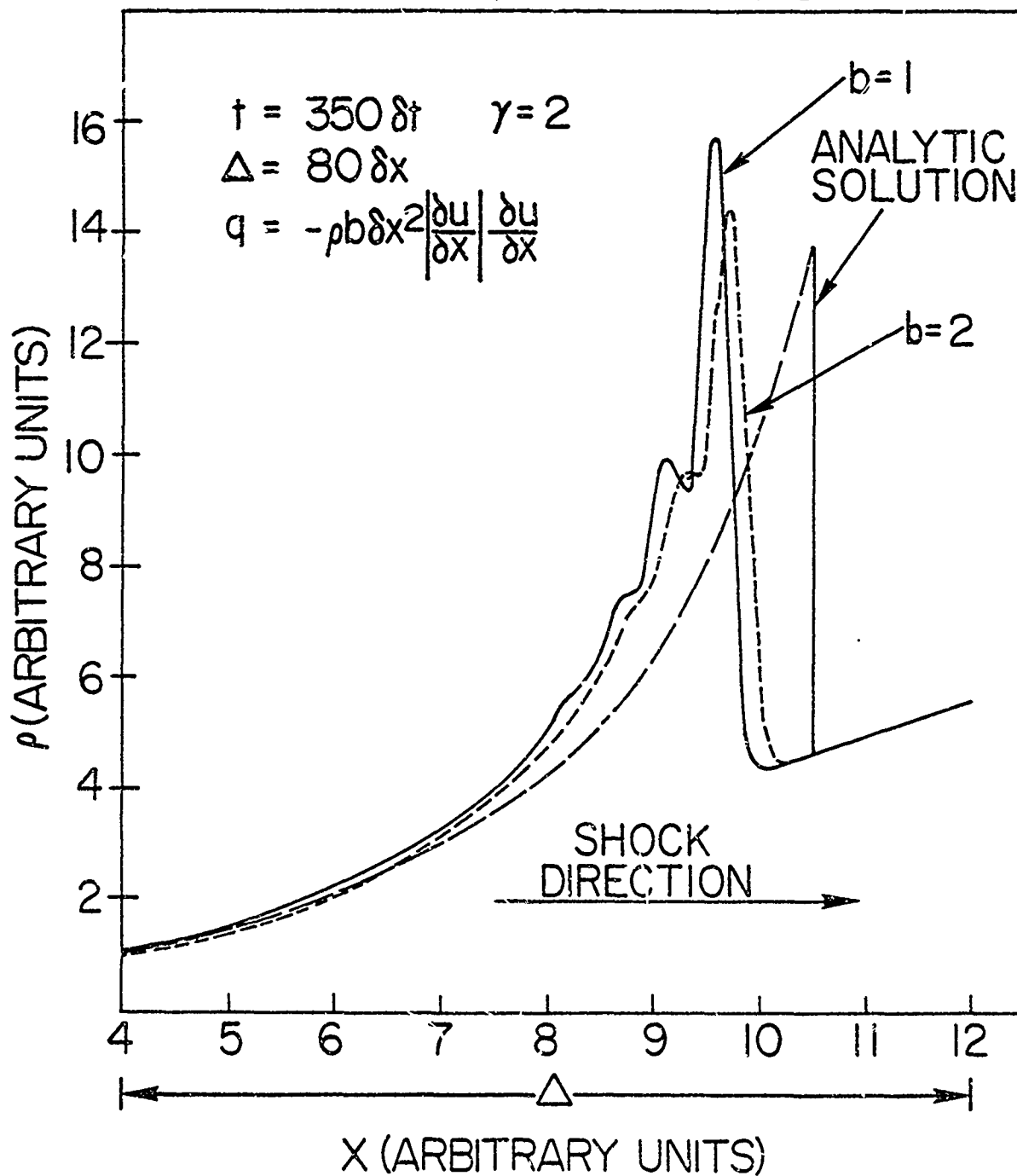


Fig. 7 — Influence of grid size. Grid size is half that used in Figs. 1 through 5. Temperature equation formulation using LW.

TEMPERATURE AND TOTAL ENERGY EQUATION - FCT ALGORITHM -

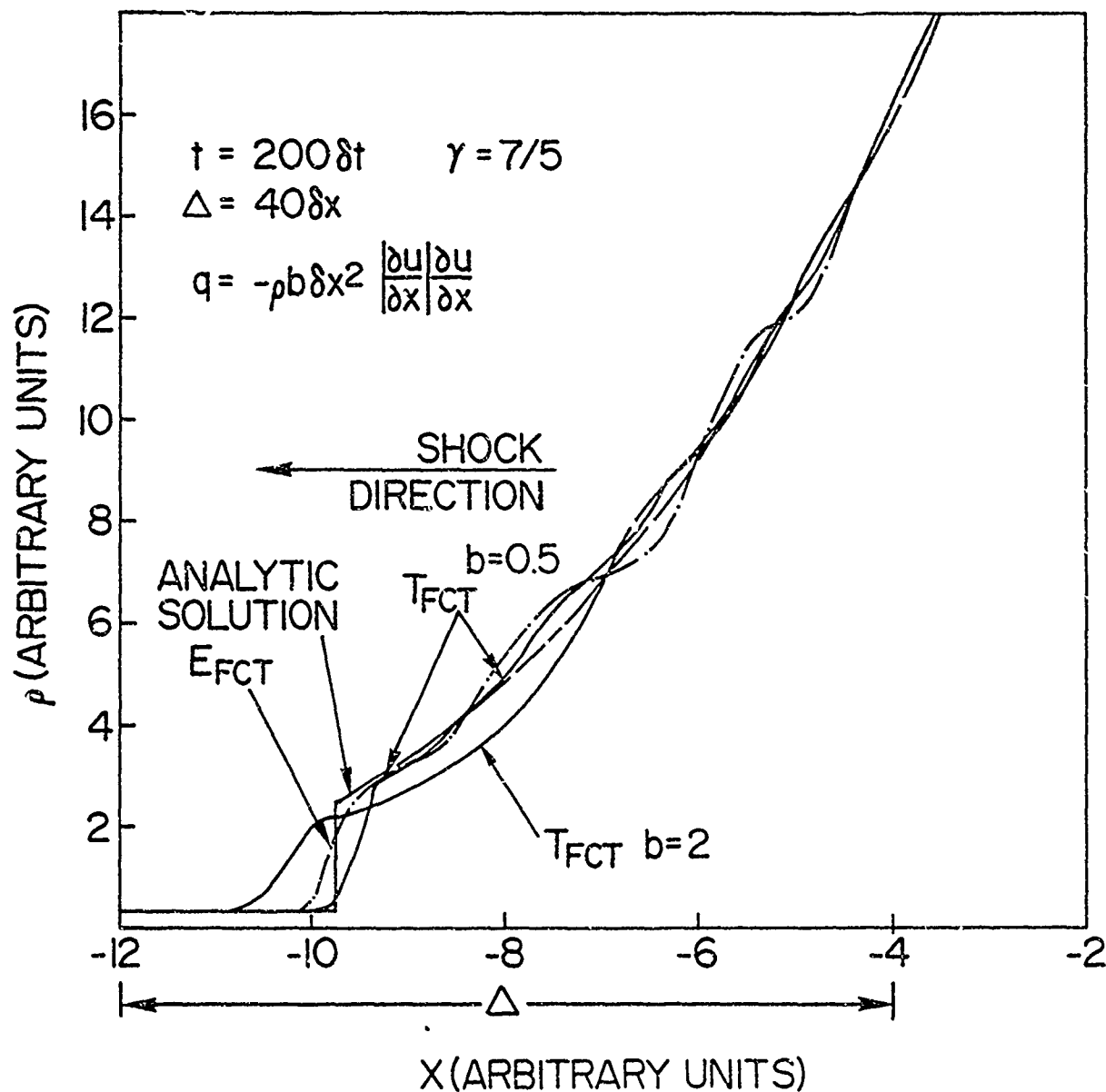


Fig. 8 — Shock density profiles for shock propagating in the decreasing density region. Temperature and energy equation formulations using FCT. The shock was located at $x = 0$ at $t = 0$.

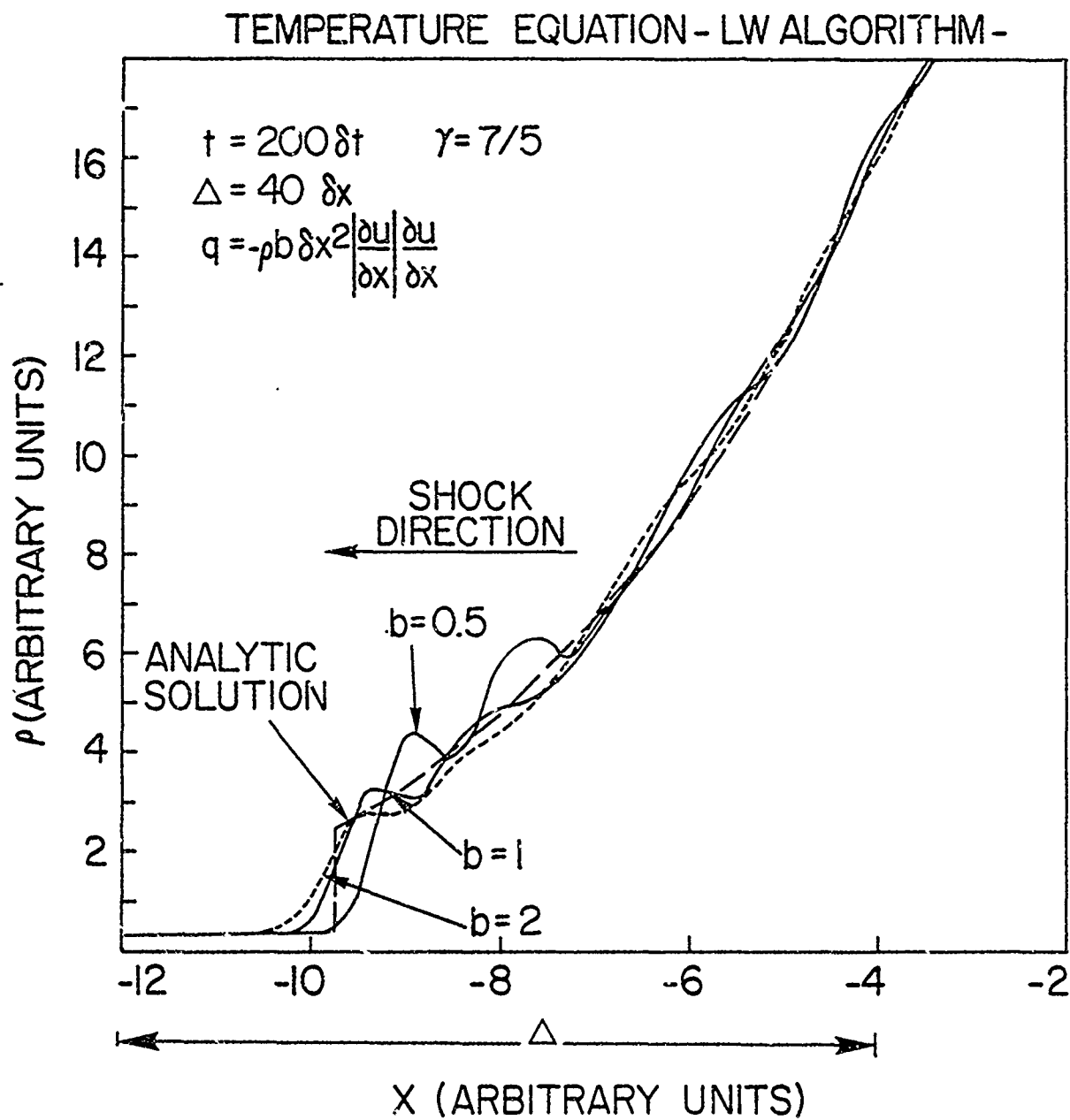


Fig. 9 — Same as Fig. 8 using LW algorithm

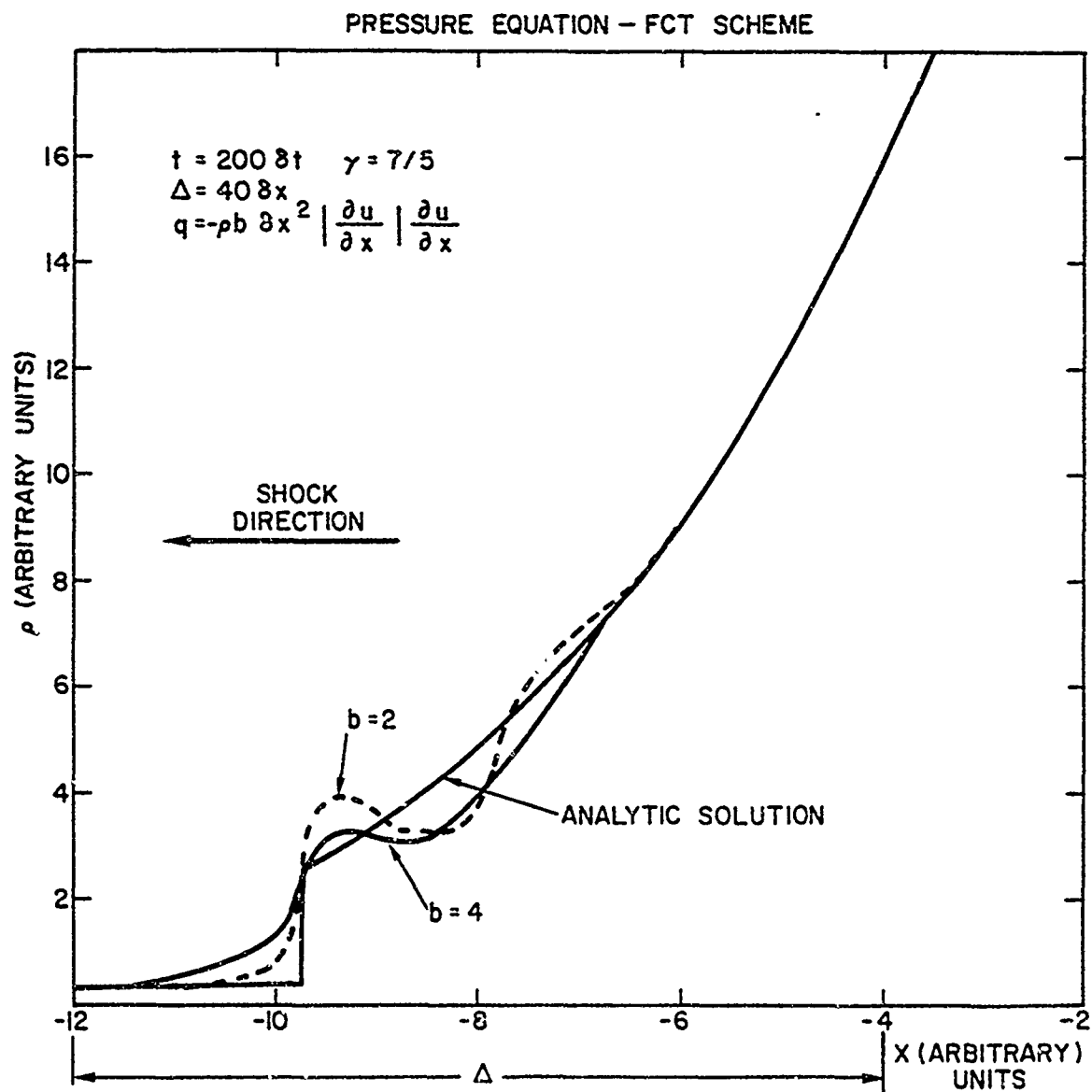


Fig. 10 — Results for the pressure equation formulation using FCT